A mechanistic study of thiol addition to N-phenylacrylamide, relating reactivity to thiol pK_a

Sarah K. I. Watt[a], Janique G. Charlebois[a], Christopher N. Rowley[b], Jeffrey W. Keillor[a]*

[a]Department of Chemistry and Biomolecular Sciences, University of Ottawa

Ottawa, Canada

[b] Department of Chemistry, Carleton University,

Ottawa, Canada

***Corresponding author:** jkeillor@uottawa.ca

Table of Contents **Page**

Table S1. pH of buffer, mobile phase gradient, length of run and retention times of NPA and thiol-adduct for each experiment of NPA with RSH (**1a-e**).

Thiol	pH of Aqueous Buffer	Mobile Phase Gradient (% CH_3CN in H_2O)	Total Length of Run (min)	Retention Time NPA (min)	Retention Time Adduct (min)
1a	7.4	20-80	15	7.9	5.7
1b	7.4	20-80	15	7.6	3.3
1c	7.4	20-80	15	7.9	3.4
1d	9.0	20-80	15	7.6	6.4
1e	9.0	20-50	20	8.7	9.9

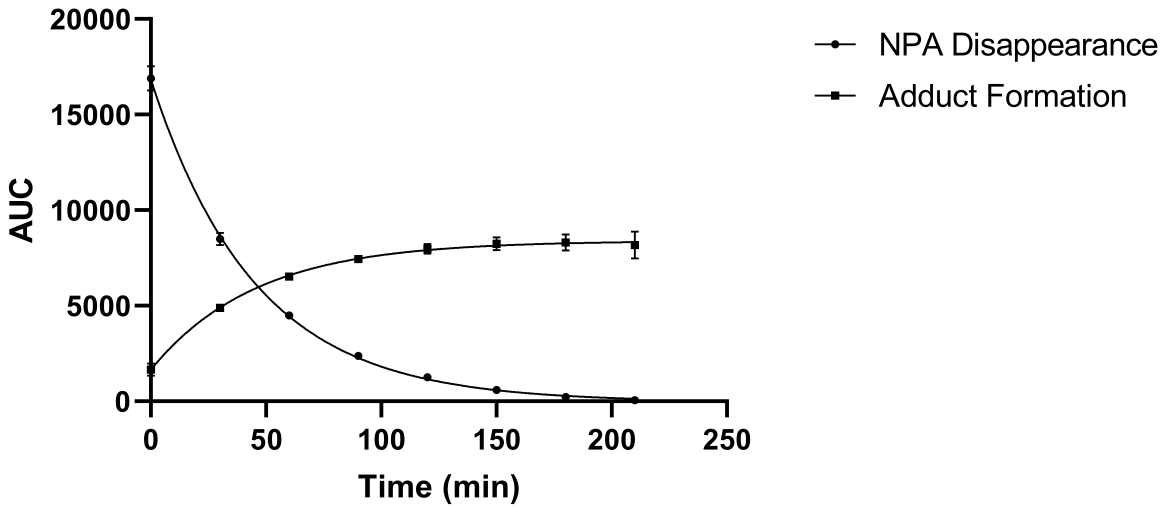

Figure S1. Plot of disappearance of NPA (1mM) and formation of adduct for the addition of DEC (10 mM) vs time (min) in 67 mM potassium phosphate buffer (1% v/v DMSO), pH 7.4, μ = 0.100, T = 22°C. The area under the curve (AUC) was integrated from the chromatograph at 214 nm for the peaks corresponding to NPA and the adduct. The AUC data for disappearance of NPA were fitted to a mono-exponential decay with the constraint that the plateau = 0 and the data for formation of adduct were fitted to a mono-exponential association to afford the k_{obs} values summarized in **Table S1**.

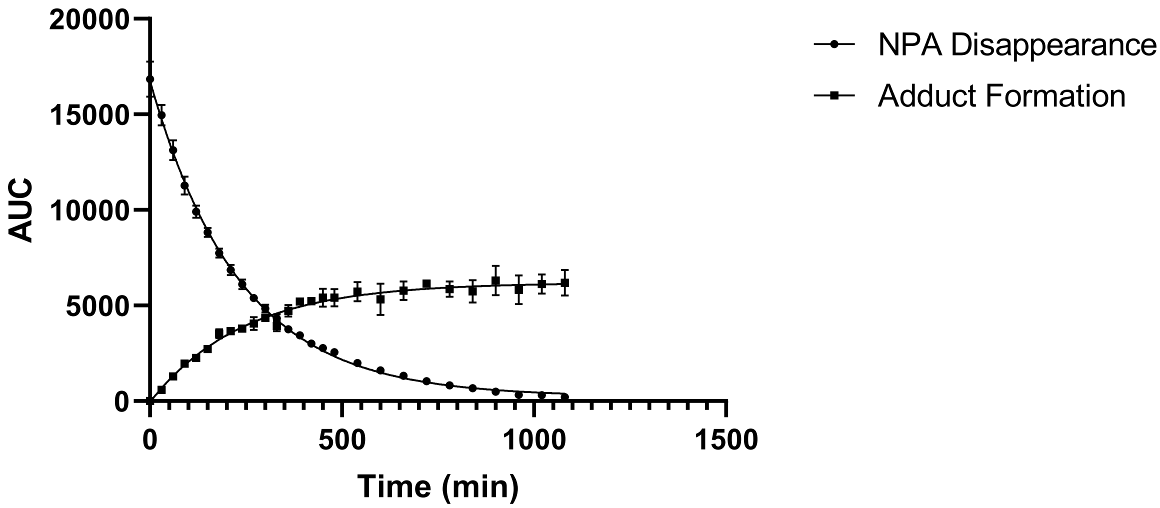

Figure S2. Plot of disappearance of NPA (1 mM) and formation of adduct for the addition of Cys (10 mM) vs time (min) in 67 mM potassium phosphate buffer (1% v/v DMSO), pH 7.4, μ = 0.100, T = 22°C. The area under the curve (AUC) was integrated from the chromatograph at 214 nm for the peaks corresponding to NPA and the adduct. The AUC data for disappearance of NPA were fitted to a mono-exponential decay with the constraint that the plateau = 0 and the data for formation of adduct were fitted to a mono-exponential association with the constraint that $Y_0 = 0$ to afford the k_{obs} values summarized in **Table S1**.

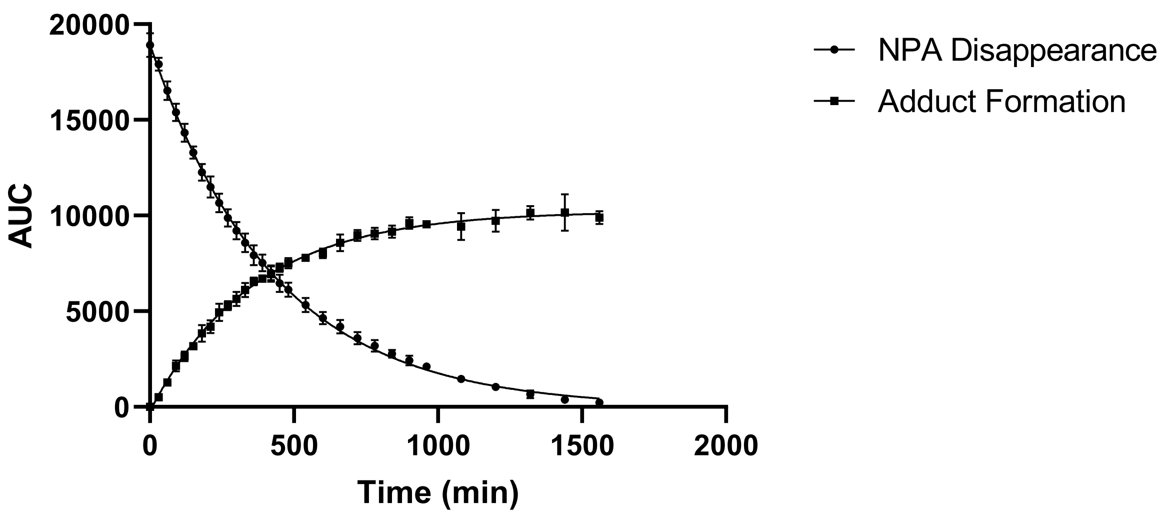

Figure S3. Plot of disappearance of NPA (1 mM) and formation of adduct for the addition of GSH (10 mM) vs time (min) in 67 mM potassium phosphate buffer (1% v/v DMSO), pH 7.4, μ = 0.100, T = 22°C. The area under the curve (AUC) was integrated from the chromatograph at 214 nm for the peaks corresponding to NPA and the adduct. The AUC data for disappearance of NPA were fitted to a mono-exponential decay with the constraint that the plateau = 0 and the data for formation of adduct were fitted to a mono-exponential association with the constraint that $Y_0 = 0$ to afford the k_{obs} values summarized in **Table S1**.

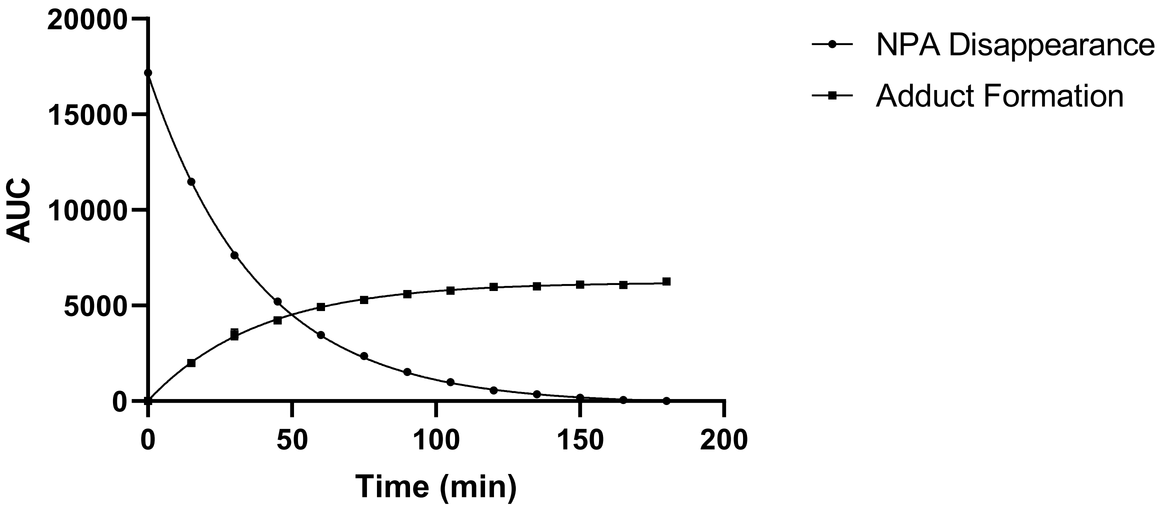

Figure S4. Plot of disappearance of NPA (1 mM) and formation of adduct for the addition of BME (10 mM) vs time (min) in 67 mM CHES buffer (1% v/v DMSO), pH 9, μ = 0.100, T = 22°C. The area under the curve (AUC) was integrated from the chromatograph at 214 nm for the peaks corresponding to NPA and the adduct. The AUC data for disappearance of NPA were fitted to a mono-exponential decay with the constraint that the plateau = 0 and the data for formation of adduct were fitted to a mono-exponential association with the constraint that Y_0 = 0 to afford the k_{obs} values summarized in **Table S1**.

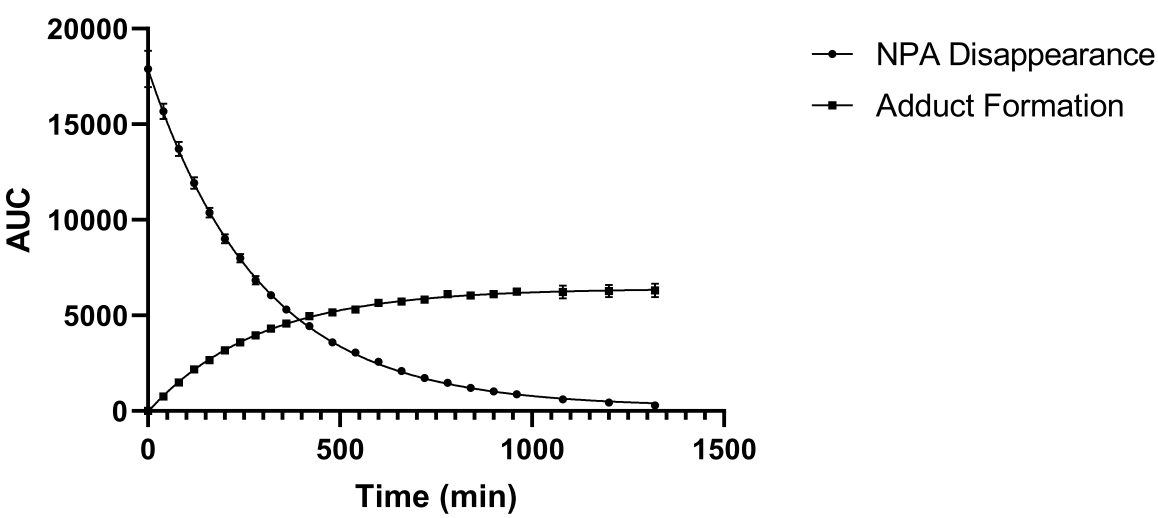

Figure S5. Plot of disappearance of NPA (1 mM) and formation of adduct for the addition of MPA (10 mM) vs time (min) in 67 mM CHES buffer (1% v/v DMSO), pH 9, μ = 0.100, T = 22°C. The area under the curve (AUC) was integrated from the chromatograph at 214 nm for the peaks corresponding to NPA and the adduct. The AUC data for disappearance of NPA were fitted to a mono-exponential decay with the constraint that the plateau = 0 and the data for formation of adduct were fitted to a mono-exponential association with the constraint that Y_0 = 0 to afford the k_{obs} values summarized in **Table S1**.

Table S2. Observed rate constants (k_{obs}), calculated second order rate constants (k_2^{calc}), and corrected second order rate constants (k_2^{corr}) for the addition of RSH (**1a-e**) to NPA. Measurements were made in duplicate for both the disappearance of acrylamide and appearance of adduct, unless otherwise indicated. Errors represent the standard deviation of the replicate values.

Thiol	k_{obs} (s^{-1})	k_2^{calc} ($M^{-1}s^{-1}$)	k_2^{corr} ($M^{-1}s^{-1}$)	$\log(k_2^{corr})$
1a	0.37 ± 0.03[a]	0.037 ± 0.003	0.13 ± 0.01	-0.887 ± 0.036
1b	0.068 ± 0.007	0.0068 ± 0.0007	0.061 ± 0.006	-1.214 ± 0.043
1c	0.041 ± 0.002[b]	0.0041 ± 0.0002	0.086 ± 0.005	-1.064 ± 0.024
1d	0.44 ± 0.02	0.044 ± 0.002	0.220 ± 0.008	-0.657 ± 0.016
1e	0.056 ± 0.002	0.0056 ± 0.0002	0.118 ± 0.004	-0.929 ± 0.013

[a]Measurements made in triplicate. [b]Measurements made in quadruplet.

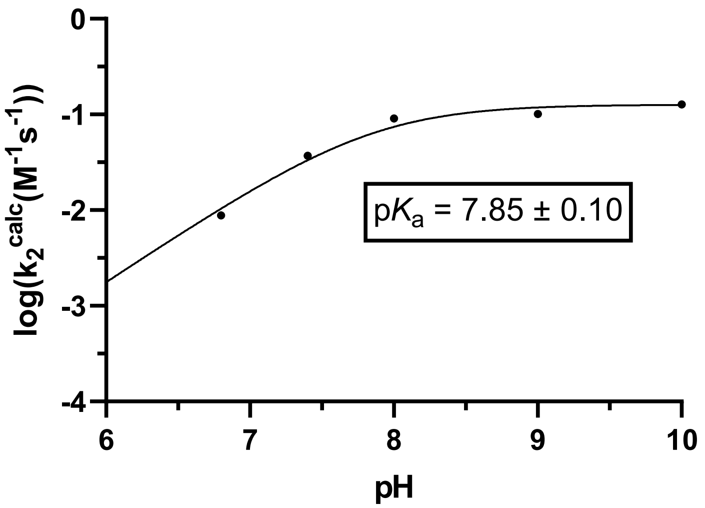

Figure S6. Plot of log (k_2^{calc}) vs pH for the addition of 1a to NPA in aqueous buffer (1% v/v DMSO), μ = 0.100, T = 22°C. The data were fitted to the **eq 1**, giving a kinetic pK_a value of 7.85 ± 0.10.

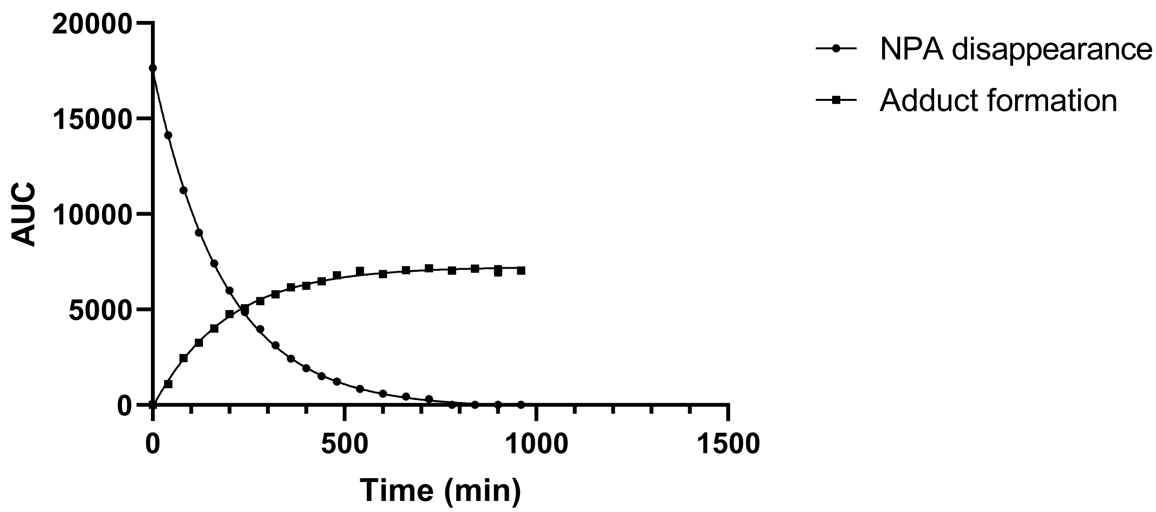

Figure S7. Plot of disappearance of NPA (1 mM) and formation of adduct for the addition of 1a (10 mM) vs time (min) in 67 mM MOPS buffer (1% v/v DMSO) at pH 6.8, μ = 0.100, T = 22°C. The area under the curve (AUC) was integrated from the chromatograph at 214 nm for the peaks corresponding to NPA and the adduct. The AUC data for disappearance of NPA were fitted to a mono-exponential decay with the constraint that the plateau = 0 and the data for formation of adduct were fitted to a mono-exponential association with the constraint that Y_0 = 0 to afford the k_{obs} values summarized in **Table S2**.

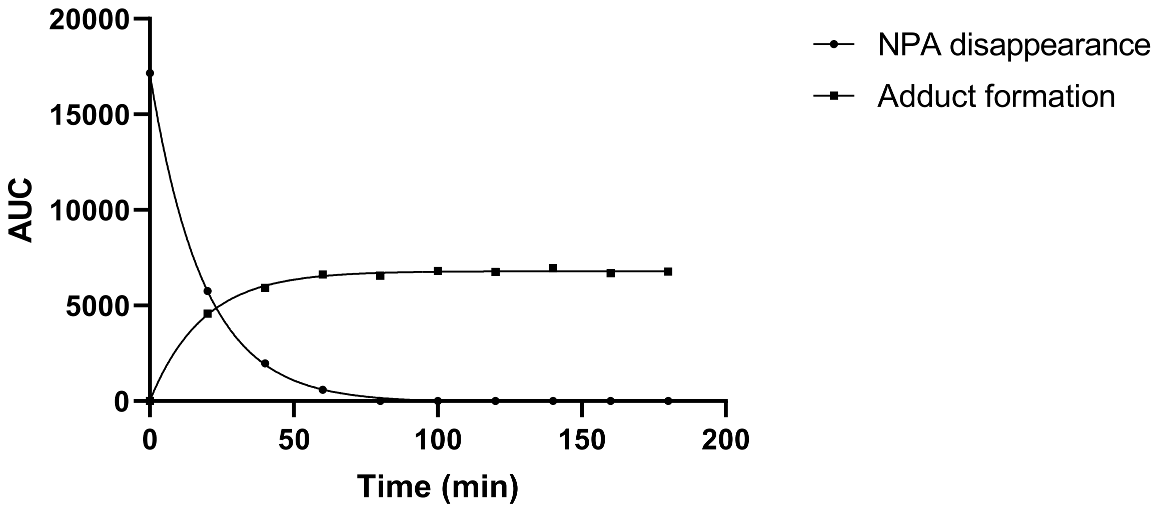

Figure S8. Plot of disappearance of NPA (1 mM) and formation of adduct for the addition of 1a (10 mM) vs time (min) in 67 mM TRIS buffer (1% v/v DMSO) at pH 8.0, μ = 0.100, T = 22°C. The area under the curve (AUC) was integrated from the chromatograph at 214 nm for the peaks corresponding to NPA and the adduct. The AUC data for disappearance of NPA were fitted to a mono-exponential decay with the constraint that the plateau = 0 and the data for formation of adduct were fitted to a mono-exponential association with the constraint that Y_0 = 0 to afford the k_{obs} values summarized in **Table S2**.

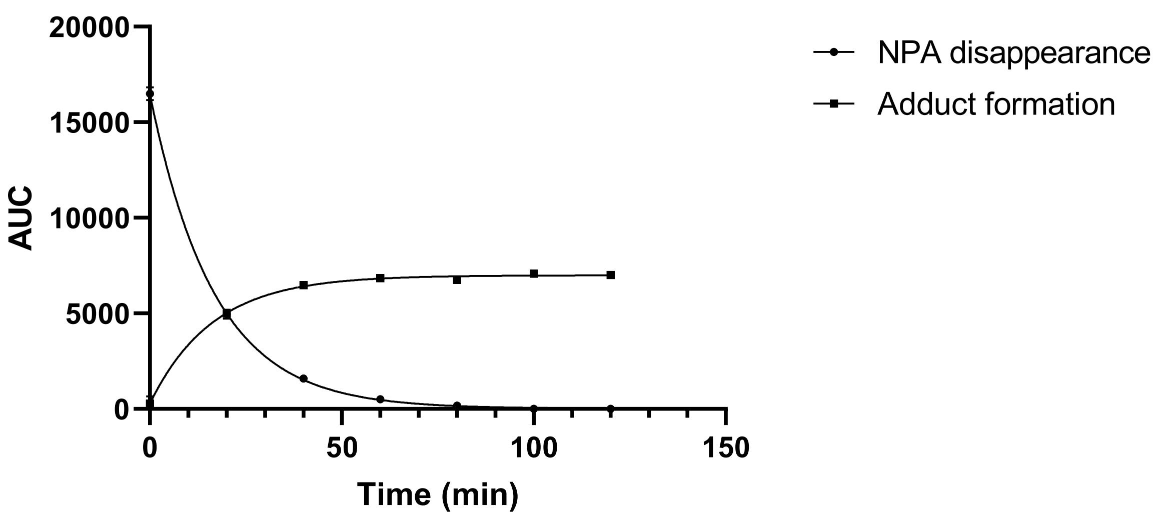

Figure S9. Plot of disappearance of NPA (1 mM) and formation of adduct for the addition of 1a (10 mM) vs time (min) in 67 mM CHES buffer (1% v/v DMSO) at pH 9.0, μ = 0.100, T = 22°C. The area under the curve (AUC) was integrated from the chromatograph at 214 nm for the peaks corresponding to NPA and the adduct. The AUC data for disappearance of NPA were fitted to a mono-exponential decay with the constraint that the plateau = 0 and the data for formation of adduct were fitted to a mono-exponential association with the constraint that Y_0 = 0 to afford the k_{obs} values summarized in **Table S2**.

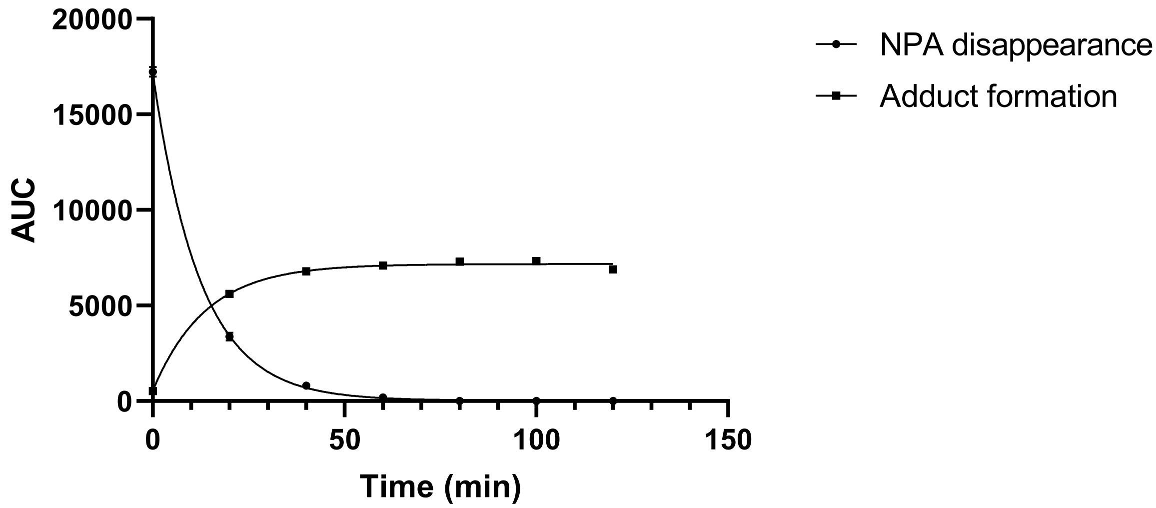

Figure S10. Plot of disappearance of NPA (1 mM) and formation of adduct for the addition of 1a (10 mM) vs time (min) in 67 mM CAPS buffer (1% v/v DMSO) at pH 10.0, $\mu = 0.100$, T = 22°C. The area under the curve (AUC) was integrated from the chromatograph at 214 nm for the peaks corresponding to NPA and the adduct. The AUC data for disappearance of NPA were fitted to a mono-exponential decay with the constraint that the plateau = 0 and the data for formation of adduct were fitted to a mono-exponential association with the constraint that $Y_0 = 0$ to afford the k_{obs} values summarized in **Table S2**.

Table S3. Observed rate constants (k_{obs}) and calculated second order rate constants (k_2^{calc}) for the addition of RSH (**1a**) to NPA at variable pH. Measurements were made in duplicate for both the disappearance of acrylamide and appearance of adduct. Errors represent the standard deviation of the replicate values.

pH	k_{obs} (s^{-1})	k_2^{calc} ($M^{-1}s^{-1}$)	log(k_2^{calc})
6.8	0.088 ± 0.004	0.0088 ± 0.0004	-2.056 ± 0.020
7.4	0.369 ± 0.032	0.0369 ± 0.0032	-1.433 ± 0.036
8.0	0.908 ± 0.033	0.0908 ± 0.0033	-1.042 ± 0.016
9.0	1.010 ± 0.044	0.1010 ± 0.0044	-0.996 ± 0.019
10.0	1.280 ± 0.085	0.1280 ± 0.0085	-0.894 ± 0.029

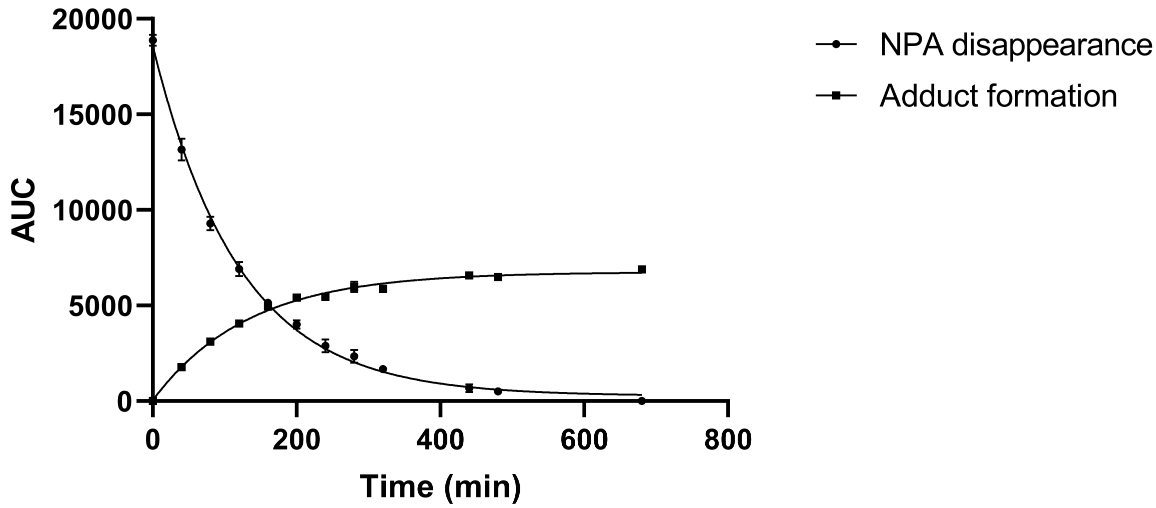

Figure S11. Plot of disappearance of NPA (1 mM) and formation of adduct for the addition of 1e (10 mM) vs time (min) in 67 mM CHES buffer (1% v/v DMSO) at pH 9.0, μ = 0.100, T = 37°C. The area under the curve (AUC) was integrated from the chromatograph at 214 nm for the peaks corresponding to NPA and the adduct. The AUC data for disappearance of NPA were fitted to a mono-exponential decay with the constraint that the plateau = 0 and the data for formation of adduct were fitted to a mono-exponential association with the constraint that $Y_0 = 0$ to afford the k_{obs} values summarized in **Table S3**.

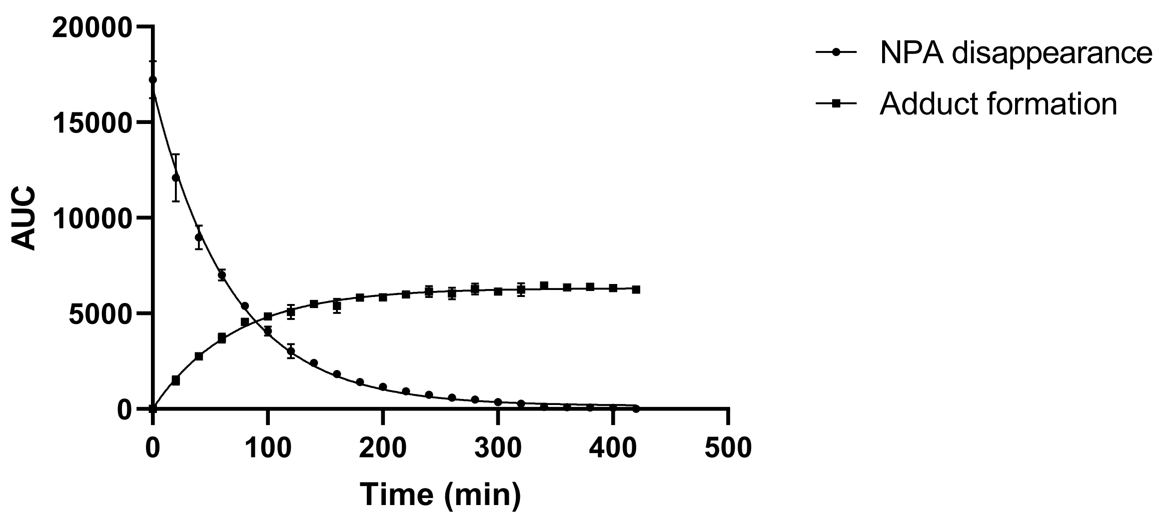

Figure S12. Plot of disappearance of NPA (1 mM) and formation of adduct for the addition of 1e (10 mM) vs time (min) in 67 mM CHES buffer (1% v/v DMSO) at pH 9.0, μ = 0.100, T = 53°C. The area under the curve (AUC) was integrated from the chromatograph at 214 nm for the peaks corresponding to NPA and the adduct. The AUC data for disappearance of NPA were fitted to a mono-exponential decay with the constraint that the plateau = 0 and the data for formation of adduct were fitted to a mono-exponential association with the constraint that $Y_0 = 0$ to afford the k_{obs} values summarized in **Table S3**.

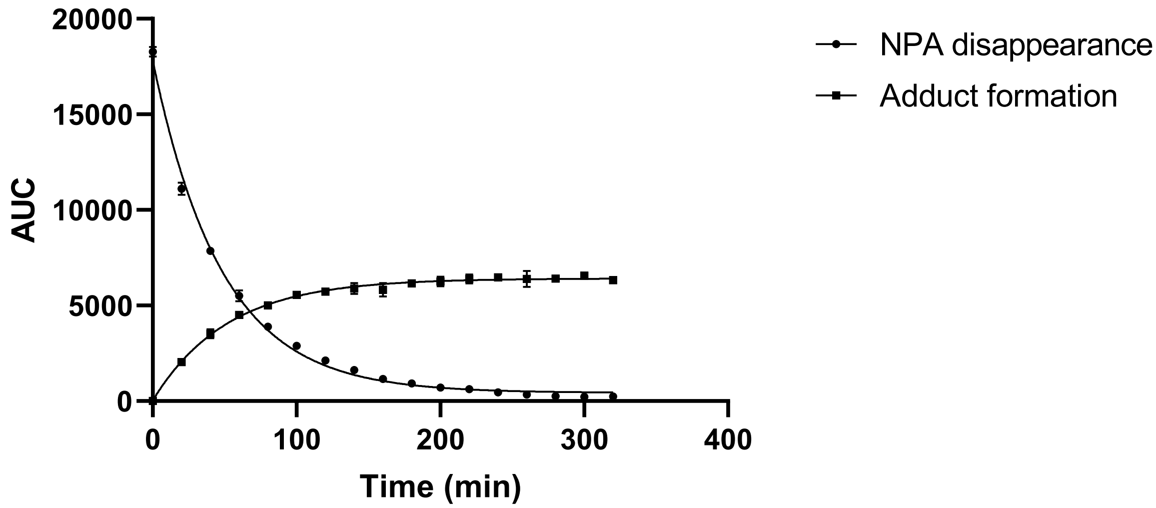

Figure S13. Plot of disappearance of NPA (1 mM) and formation of adduct for the addition of 1e (10 mM) vs time (min) in 67 mM CHES buffer (1% v/v DMSO) at pH 9.0, μ = 0.100, T = 62°C. The area under the curve (AUC) was integrated from the chromatograph at 214 nm for the peaks corresponding to NPA and the adduct. The AUC data for disappearance of NPA were fitted to a mono-exponential decay with the constraint that the plateau = 0 and the data for formation of adduct were fitted to a mono-exponential association with the constraint that Y_0 = 0 to afford the k_{obs} values summarized in **Table S3**.

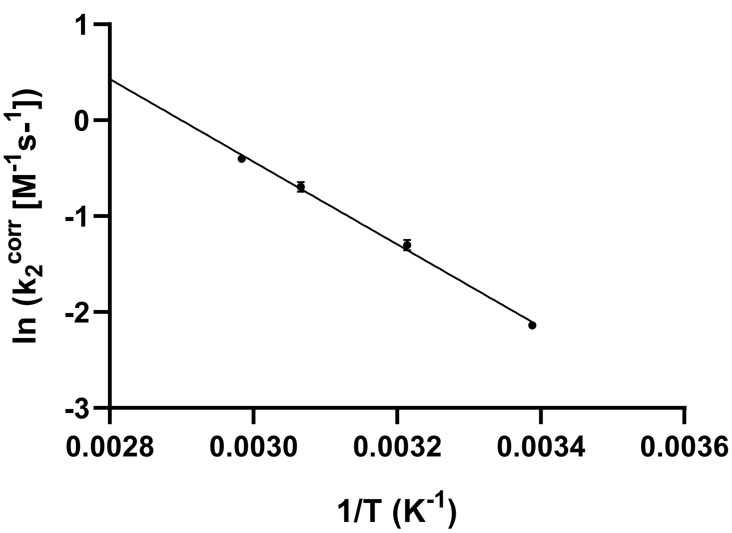

Figure S14. Arrhenius plot showing ln(k_2^{corr}) vs 1/T for the addition of 1e to NPA in 67 mM CHES buffer (1% v/v DMSO), pH = 9.0, μ = 0.100. The data were fitted to a linear regression to obtain a slope of -4308 ± 173.3 and y-intercept of 12.49 ± 0.55.

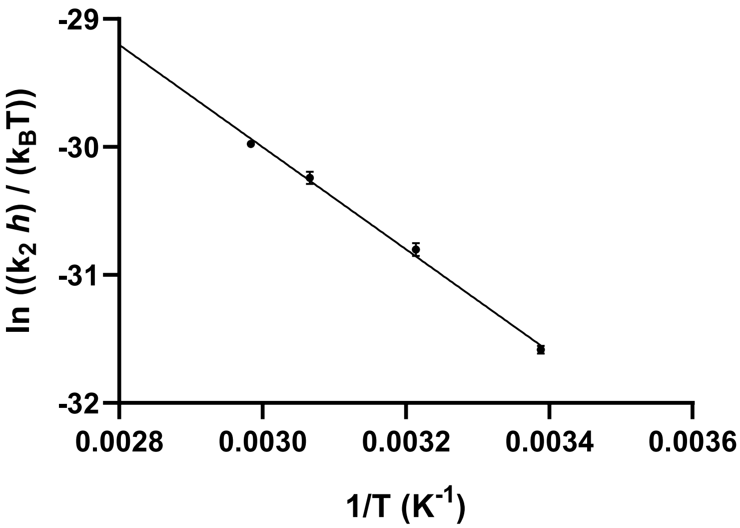

Figure S15. Eyring plot showing $\ln((k_2 h)/(k_B T))$ vs 1/T for the addition of 1e to NPA in 67 mM CHES buffer (1% v/v DMSO), pH = 9.0, μ = 0.100. The data were fitted to a linear regression to obtain a slope of -3994 ± 177.2 and y-intercept of -18.02 ± 0.56.

Table S4. Observed rate constants (k_{obs}), calculated second order rate constants (k_2^{calc}), and corrected second order rate constants (k_2^{corr}) for the addition of MPA (**1e**) to NPA at variable temperatures. Measurements were made in duplicate for both the disappearance of acrylamide and appearance of adduct. Errors represent the standard deviation of the replicate values.

Temp (°C)	k_{obs} (s^{-1})	k_2^{calc} ($M^{-1}s^{-1}$)	k_2^{corr} ($M^{-1}s^{-1}$)	$\ln(k_2^{corr})$	$\ln((k_2^{corr}h)/k_BT)$
22	0.056 ± 0.002	0.0056 ± 0.0002	0.118 ± 0.004	-2.137 ± 0.029	-31.584 ± 0.031
38	0.130 ± 0.007	0.013 ± 0.0007	0.272 ± 0.015	-1.302 ± 0.053	-30.802 ± 0.050
52	0.238 ± 0.012	0.024 ± 0.001	0.499 ± 0.025	-0.695 ± 0.050	-30.242 ± 0.050
63	0.320 ± 0.007	0.032 ± 0.0006	0.670 ± 0.014	-0.401 ± 0.021	-29.975 ± 0.021

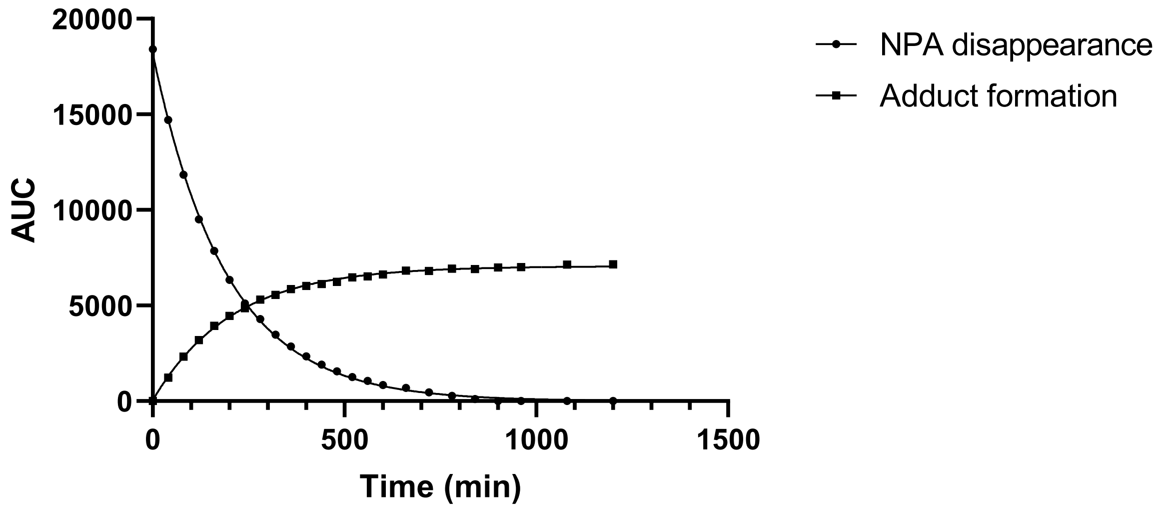

Figure S16. Plot of disappearance of NPA (1 mM) and formation of adduct for the addition of 1e (10 mM) vs time (min) in 67 mM CHES buffer (1% v/v DMSO), pH 9.0, μ = 0.050, T = 22°C. The area under the curve (AUC) was integrated from the chromatograph at 214 nm for the peaks corresponding to NPA and the adduct. The AUC data for disappearance of NPA were fitted to a mono-exponential decay with the constraint that the plateau = 0 and the data for formation of adduct were fitted to a mono-exponential association with the constraint that Y_0 = 0 to afford the k_{obs} values summarized in **Table S4**.

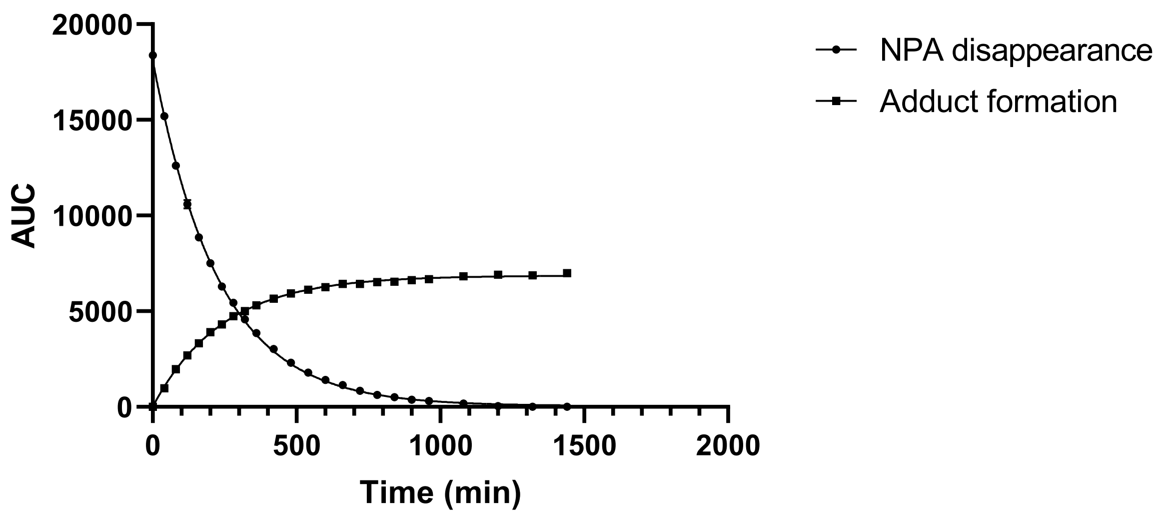

Figure S17. Plot of disappearance of NPA (1 mM) and formation of adduct for the addition of 1e (10 mM) vs time (min) in 67 mM CHES buffer (1% v/v DMSO), pH 9.0, μ = 0.075, T = 22°C. The area under the curve (AUC) was integrated from the chromatograph at 214 nm for the peaks corresponding to NPA and the adduct. The AUC data for disappearance of NPA were fitted to a mono-exponential decay with the constraint that the plateau = 0 and the data for formation of adduct were fitted to a mono-exponential association with the constraint that Y_0 = 0 to afford the k_{obs} values summarized in **Table S4**.

Table S5. Observed rate constants (k_{obs}), calculated second order rate constants (k_2^{calc}), and corrected second order rate constants (k_2^{corr}) for the addition of MPA (**1e**) to NPA at varying ionic strengths. Measurements were made in duplicate for both the disappearance of acrylamide and appearance of adduct. Errors represent the standard deviation of the replicate values.

[KCl] (M)	**k_{obs} (s^{-1})**	**k_2^{calc} ($M^{-1}s^{-1}$)**	**k_2^{corr} ($M^{-1}s^{-1}$)**
0.050	0.0845 ± 0.0032	0.00845 ± 0.00032	0.177 ± 0.007
0.075	0.0707 ± 0.0024	0.00707 ± 0.00024	0.148 ± 0.005
0.100	0.0562 ± 0.0017	0.00562 ± 0.00017	0.118 ± 0.004

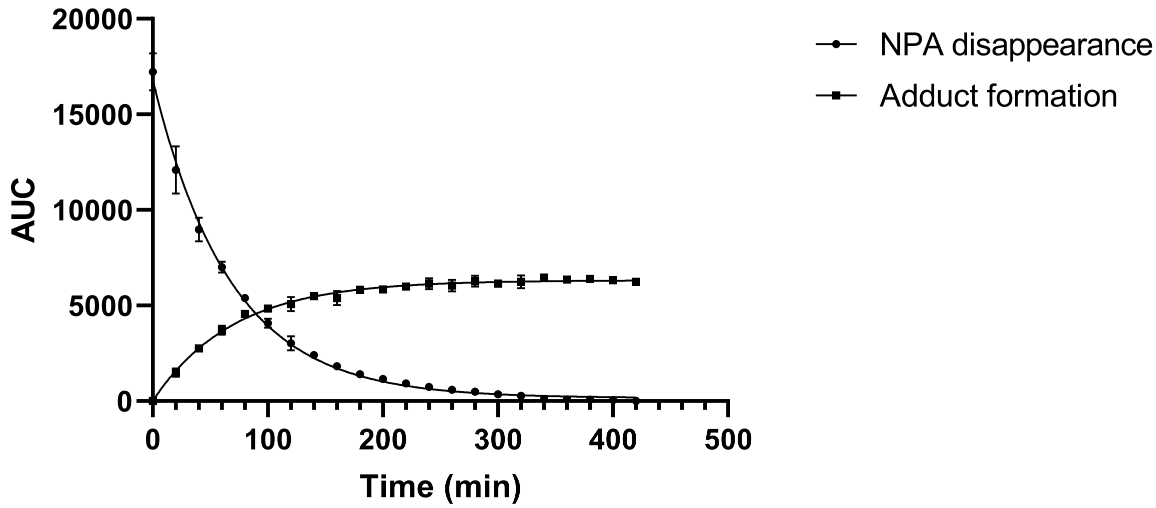

Figure S18. Plot of disappearance of NPA (1 mM) and formation of adduct for the addition of 1e (10 mM) vs time (min) in carbonate buffer prepared in D_2O (1% v/v ACN), pD = 9.7, μ = 0.100, T = 22°C. The area under the curve (AUC) was integrated from the chromatograph at 214 nm fort eh peaks corresponding to NPA and the adduct. The AUC data for disappearance of NPA were fitted to a mono-exponential decay with the constraint that the plateau = 0 and the data for formation of adduct were fitted to a mono-exponential association with the constraint that Y_0 = 0 to afford the k_{obs} values summarized in **Table S5**.

Table S6. Observed rate constants (k_{obs}), calculated second order rate constants (k_2^{calc}), corrected second order rate constants (k_2^{corr}), and calculated solvent kinetic isotope effect ratio for the addition of MPA (**1e**) to NPA. Measurements were made in duplicate for both the disappearance of acrylamide and appearance of adduct. Errors represent the standard deviation of the replicate values.

L_2O	k_{obs} (s^{-1})	k_2^{calc} ($M^{-1}s^{-1}$)	k_2^{corr} ($M^{-1}s^{-1}$)	$k_2^{corr,H2O}/k_2^{corr,D2O}$
H	0.0562 ± 0.0017	0.00562 ± 0.00017	0.118 ± 0.004	1.09 ± 0.04
D	0.103 ± 0.003	0.0103 ± 0.0003	0.108 ± 0.003	

Figure S19. ^{1}H-NMR spectra of adduct formed on reaction of MPA with NPA in D_2O.

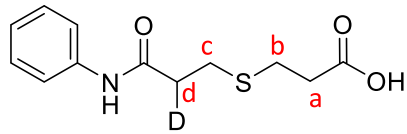

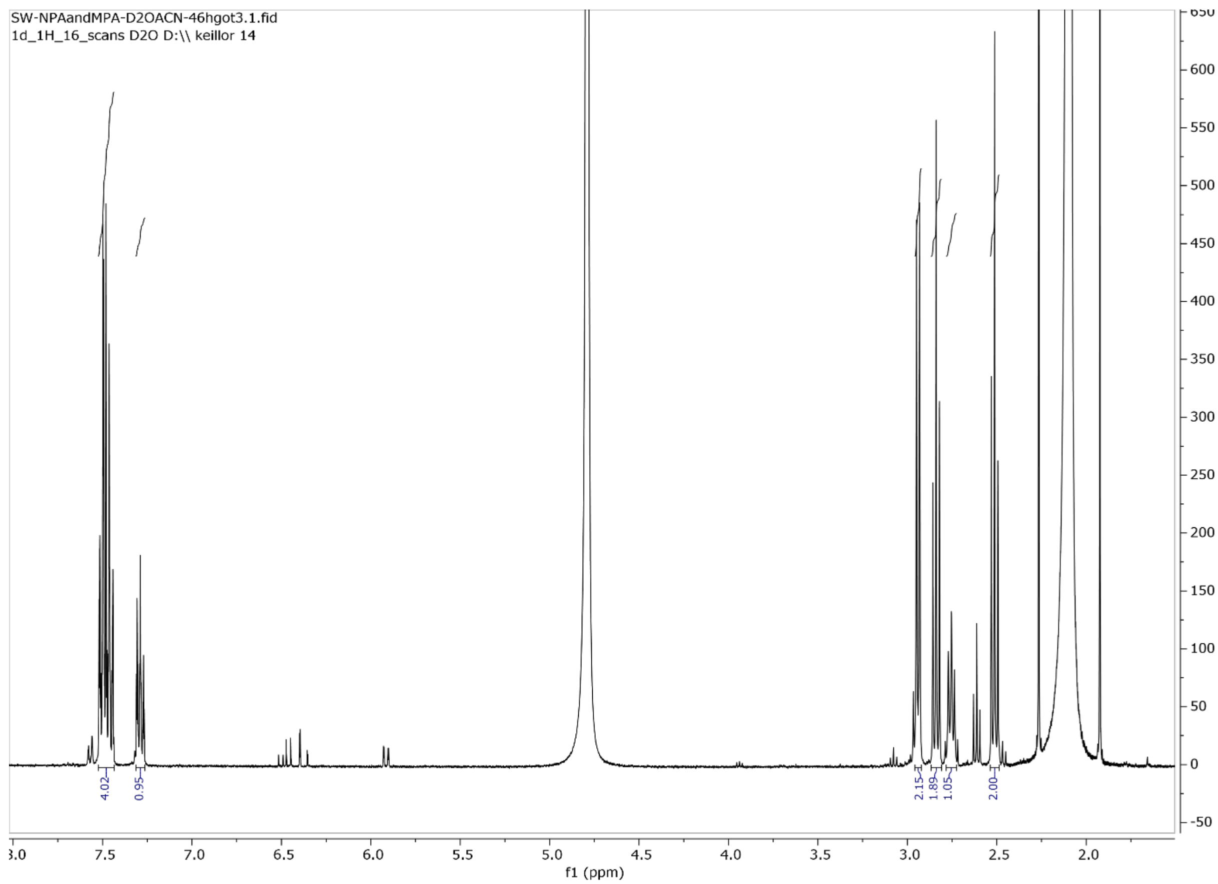

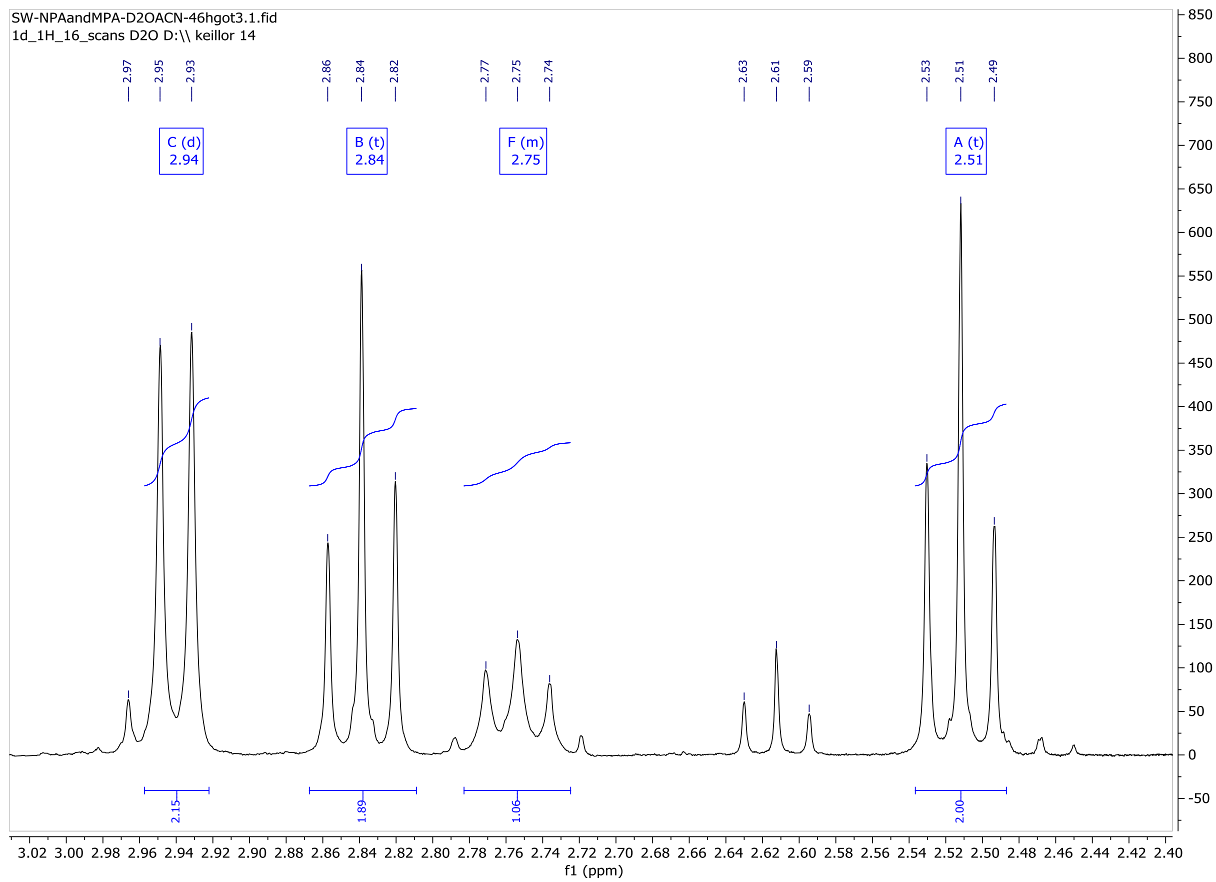
SW-NPAandMPA-D2OACN-46hgot3.1.fid
1d_1H_16_scans D2O D:\\ keillor 14
C (d)
2.94
B (t)
2.84
F (m)
2.75
A (t)
2.51
2.15
1.89
1.06
2.00
f1 (ppm)

Figure S20: COSY spectrum of adduct formed on reaction of MPA with NPA in D_2O.

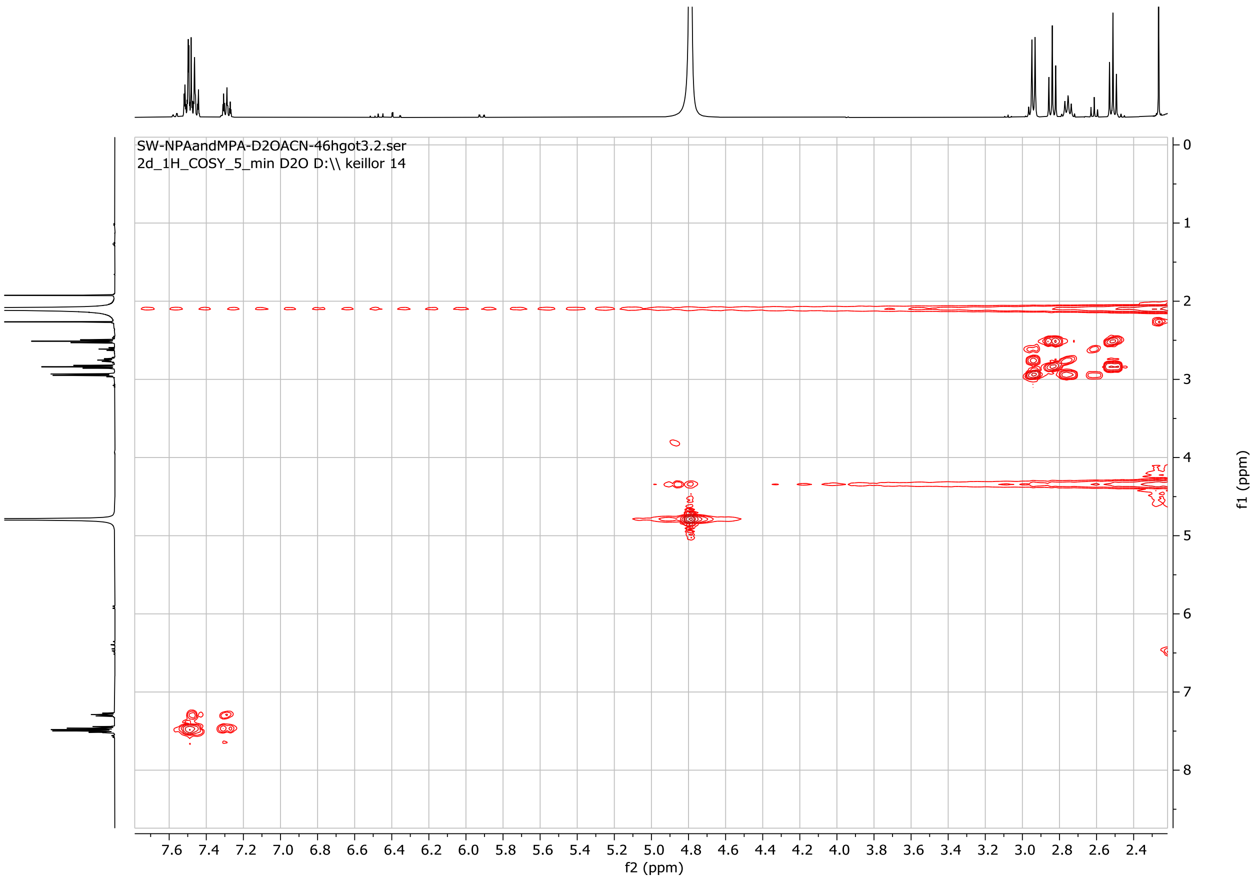

Methanethiol (HF=-438.7161991, NImag=0)

C	-1.149875	0.019721	0.000000
H	-1.521320	-1.004113	-0.000000
H	-1.511252	0.526248	-0.892471
H	-1.511252	0.526248	0.892472
S	0.658342	-0.087240	0.000000
H	0.909595	1.229124	0.000000

Methanethiolate (HF=-438.2236907, NImag=0)

C	0.000000	0.000000	-1.122213
H	0.000000	1.015846	-1.529501
H	-0.879748	-0.507923	-1.529501
H	0.879748	-0.507923	-1.529501
S	-0.000000	-0.000000	0.707611

N-Phenylacrylamide (HF=-478.3703966, NImag=0)

C	3.611710	-1.057555	0.511104
H	2.943491	-1.687752	1.087579
C	3.196285	0.005129	-0.163180
H	3.899237	0.636878	-0.693779
C	1.799390	0.510568	-0.209297
O	1.587295	1.701990	-0.426736
N	0.824035	-0.405284	-0.009116
H	1.117902	-1.369748	0.014188
C	-0.569202	-0.208055	0.010601
C	-1.371784	-1.312387	-0.271567
C	-1.162741	1.009409	0.331819
C	-2.750400	-1.199130	-0.243131
H	-0.905735	-2.260536	-0.513364

C	-2.546679	1.111531	0.350031
H	-0.553845	1.866461	0.572571
C	-3.347123	0.016745	0.062630
H	-3.360050	-2.065916	-0.465224
H	-2.999592	2.062864	0.600122
H	-4.425523	0.107605	0.080544
H	4.660775	-1.326323	0.521009

Transition State 1 (HF=-916.5980778,NImag=1)

C	-2.727797	0.851973	-1.013713
H	-2.207420	0.519948	-1.900693
C	-2.080776	1.625548	-0.071959
H	-2.644296	2.239193	0.619734
C	-0.671971	1.542937	0.176270
O	-0.045133	2.351146	0.892075
N	-0.045223	0.455867	-0.404303
H	-0.680212	-0.312430	-0.619163
C	1.290990	0.078931	-0.230859
C	1.581322	-1.280803	-0.108799
C	2.339597	0.998132	-0.231149
C	2.891165	-1.712022	0.018433
H	0.767313	-1.997348	-0.115973
C	3.646755	0.556727	-0.090002
H	2.134338	2.051444	-0.352629
C	3.933580	-0.795304	0.036583
H	3.095901	-2.771609	0.110617
H	4.451022	1.282407	-0.090190
H	4.957278	-1.130959	0.141980
H	-3.791777	0.991548	-1.148428

S	-2.838250	-1.464237	-0.339721
C	-2.390145	-1.207362	1.385045
H	-3.188602	-1.511813	2.063776
H	-1.480812	-1.749675	1.651576
H	-2.199425	-0.135692	1.549347

Enolate intermediate (HF=-916.609191, NImag=0)

C	-2.601821	0.459994	-1.081563
H	-2.048393	0.188402	-1.985195
C	-1.895894	1.449839	-0.230996
H	-2.480458	2.248619	0.209289
C	-0.570338	1.377295	0.138317
O	0.058783	2.244058	0.834645
N	0.128672	0.214691	-0.281346
H	-0.456169	-0.607736	-0.336465
C	1.480567	-0.049635	-0.123602
C	1.888285	-1.370192	0.101229
C	2.466167	0.935822	-0.247493
C	3.230963	-1.692528	0.203745
H	1.135427	-2.145108	0.195617
C	3.806623	0.603379	-0.128703
H	2.177516	1.957549	-0.444550
C	4.204314	-0.707698	0.097427
H	3.516719	-2.723304	0.376383
H	4.551591	1.384189	-0.227099
H	5.253808	-0.958072	0.184410
H	-3.566665	0.853870	-1.401512
S	-2.954386	-1.214978	-0.337209
C	-3.749863	-0.723380	1.198678
H	-4.682050	-0.191465	1.003308

H	-3.970368	-1.629144	1.763181
H	-3.085759	-0.090825	1.788007

Product (HF=-917.1271492,NImag=0)

C	-2.757135	0.311344	0.070894
H	-2.799026	1.145112	-0.630138
C	-1.550151	-0.562626	-0.209756
H	-1.593037	-0.962891	-1.227071
C	-0.245318	0.195474	-0.080425
O	-0.199322	1.416489	0.009391
N	0.848269	-0.603619	-0.090987
H	0.661027	-1.594797	-0.121901
C	2.210508	-0.263251	-0.028946
C	2.691849	1.040777	-0.119371
C	3.113842	-1.317436	0.115218
C	4.059877	1.271217	-0.058089
H	2.009627	1.866266	-0.238488
C	4.473651	-1.073221	0.172280
H	2.739930	-2.332571	0.181382
C	4.957433	0.225991	0.088229
H	4.421606	2.289535	-0.129489
H	5.158422	-1.904509	0.284207
H	6.021472	0.418753	0.134341
H	-2.709159	0.716287	1.082762
S	-4.272549	-0.664633	-0.096759
C	-5.479475	0.620649	0.266039
H	-5.409606	1.433236	-0.457341
H	-6.468835	0.169222	0.196771
H	-5.338681	1.012155	1.273723
H	-1.526752	-1.421752	0.464744